Joule

CellPress

Article

A Process for Capturing CO_2 from the Atmosphere

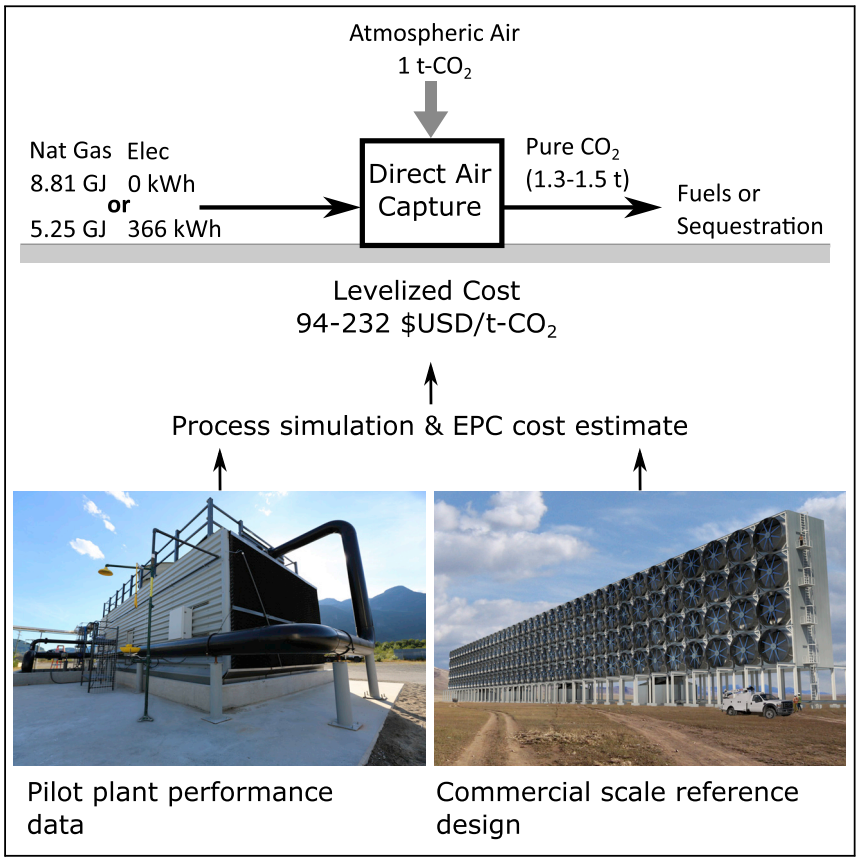

First direct air capture paper for which all major components are either drawn from well-established commercial heritage or described in sufficient detail to allow assessment by third parties. Includes energy and materials balances, commercial engineering cost breakdown, and pilot plant data. When CO_2 is delivered at 15 MPa, the design requires either 8.81 GJ of natural gas, or 5.25 GJ of gas and 366 kWhr of electricity, per ton of CO_2 captured. Levelized cost per t-CO_2 from atmosphere ranges from 94 to 232 $/t-$CO_2$.

David W. Keith, Geoffrey Holmes, David St. Angelo, Kenton Heidel

keith@carbonengineering.com

HIGHLIGHTS

Detailed engineering and cost analysis for a 1 Mt-CO_2/year direct air capture plant

Levelized costs of $94 to $232 per ton CO_2 from the atmosphere

First DAC paper with commercial engineering cost breakdown

Full mass and energy balance with pilot plant data for each unit operation

Keith et al., Joule 2, 1573–1594
August 15, 2018 © 2018 The Author(s).
Published by Elsevier Inc.
https://doi.org/10.1016/j.joule.2018.05.006

Joule

CellPress

Article

A Process for Capturing CO_2 from the Atmosphere

David W. Keith,[1,2,3,4,*] Geoffrey Holmes,[3] David St. Angelo,[3] and Kenton Heidel[3]

SUMMARY

We describe a process for capturing CO_2 from the atmosphere in an industrial plant. The design captures ~1 Mt-CO_2/year in a continuous process using an aqueous KOH sorbent coupled to a calcium caustic recovery loop. We describe the design rationale, summarize performance of the major unit operations, and provide a capital cost breakdown developed with an independent consulting engineering firm. We report results from a pilot plant that provides data on performance of the major unit operations. We summarize the energy and material balance computed using an Aspen process simulation. When CO_2 is delivered at 15 MPa, the design requires either 8.81 GJ of natural gas, or 5.25 GJ of gas and 366 kWhr of electricity, per ton of CO_2 captured. Depending on financial assumptions, energy costs, and the specific choice of inputs and outputs, the levelized cost per ton CO_2 captured from the atmosphere ranges from 94 to 232 $/t-$CO_2$.

INTRODUCTION

The capture of CO_2 from ambient air was commercialized in the 1950s as a pre-treatment for cryogenic air separation. In the 1960s, capture of CO_2 from air was considered as a feedstock for production of hydrocarbon fuels using mobile nuclear power plants.[1] In the 1990s, Klaus Lackner explored the large-scale capture of CO_2 as a tool for managing climate risk,[2] now commonly referred to as direct air capture (DAC).

Estimates of the cost of DAC vary widely. Cost estimates based on simple scaling relationships yield results[3–7] from 50 to 1,000 $/t$CO_2$. Uncertainty might be reduced if detailed specifications of individual DAC technologies were available. Yet, despite growing interest in carbon removal as a component of climate strategy, one thorough review,[8] many papers on DAC-to-CCS (carbon capture and storage) comparison,[9–13] specific absorbers,[14–17] or components of plausible DAC systems,[18] no prior paper provides a design and engineering cost basis for a complete DAC system for which all major components are (1) drawn from well-established commercial engineering heritage, or (2) described in sufficient detail to allow assessment by third parties. This paper aims to fill that gap.

Plausible DAC processes[19] use solid sorbents[20,21] or aqueous basic solutions[22] as the capture media. Solid sorbents offer the possibility of low energy input, low operating costs, and applicability across a wide range of scales. The challenges of solid sorbent designs are first, the need to build a very large structure at low cost while allowing the entire structure to be periodically sealed from the ambient air during the regeneration step when temperature, pressure, or humidity must be cycled. And second, the inherently conflicting demands of high sorbent performance, low cost, and long economic life in impure ambient air.

Context & Scale

An industrial process for large-scale capture of atmospheric CO_2 (DAC) serves two roles. First, as a source of CO_2 for making carbon-neutral hydrocarbon fuels, enabling carbon-free energy to be converted into high-energy-density fuels. Solar fuels, for example, may be produced at high-insolation low-cost locations from DAC-CO_2 and electrolytic hydrogen using gas-to-liquids technology enabling decarbonization of difficult-to-electrify sectors such as aviation. And second, DAC with CO_2 sequestration allows carbon removal.

The feasibility of DAC has been disputed, in part, because publications have not provided sufficient engineering detail to allow independent evaluation of costs. We provide an engineering cost basis for a commercial DAC system for which all major components are either drawn from well-established commercial heritage or described in sufficient detail to allow assessment by third parties. This design reflects roughly 100 person-years of development by Carbon Engineering.

This is an open access article under the CC BY-NC-ND license (http://creativecommons.org/licenses/by-nc-nd/4.0/).

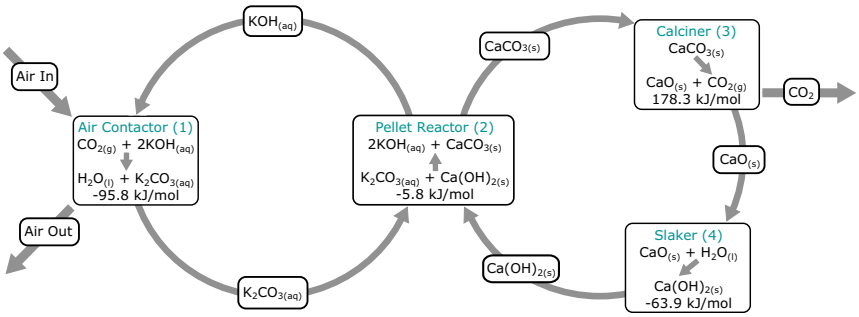

Figure 1. Process Chemistry and Thermodynamics

A calcium loop (right) drives the removal of carbonate ion and thus the regeneration of the alkali capture fluid (left). Boxes with titles show the names of the four most important unit operations. Each box shows the chemical reaction with reaction enthalpy at STP in kilojoules per mole of carbon and the reaction number for reference elsewhere in the paper. Note that water is liberated in reaction 1 and consumed in reaction 4, balancing the process. The full process has evaporative losses, as shown in Figure 2.

Aqueous sorbents offer the advantage that the contactor can operate continuously, can be built using cheap cooling-tower hardware, and the (liquid) surface is continuously renewed allowing very long contactor lifetimes despite dust and atmospheric contaminants. Once captured, CO_2 can be easily pumped to a central regeneration facility allowing economies of scale and avoiding the need to cycle conditions in the inherently large air contactor. Disadvantages of aqueous systems include the cost and complexity of the regeneration system and water loss in dry environments.

Carbon Engineering (CE) has been developing an aqueous DAC system since 2009. In 2012, we described our air-liquid contactor,[23] the front end of the process. Here, in the next section, we provide an end-to-end overview of our baseline DAC system, proceeding from a high-level description of and heat and mass balance down to descriptions of individual unit operations. The following section provides results from a 1 t-CO_2/day pilot plant operated since 2015. CE's capital cost estimating process is described in the section on Process Economics along with the levelized cost of capture under various plant configurations and economic assumptions. Finally, the Discussion provides comparison with prior literature and a discussion of options for improving the technology.

Process Description

Our process comprises two connected chemical loops (Figure 1). The first loop captures CO_2 from the atmosphere using an aqueous solution with ionic concentrations of roughly 1.0 M OH^-, 0.5 M CO_3^{2-}, and 2.0 M K^+. In the second loop, CO_3^{2-} is precipitated by reaction with Ca^{2+} to form $CaCO_3$ while the Ca^{2+} is replenished by dissolution of $Ca(OH)_2$. The $CaCO_3$ is calcined to liberate CO_2 producing CaO, which is hydrated or "slaked" to produce $Ca(OH)_2$.

CE has developed a process to implement this cycle at industrial scale. Figure 2 provides a simplified energy and material balance of the complete process (and Figure S1 shows a rendering of one possible configuration of plant equipment to perform this process). At full capacity, this plant captures 0.98 Mt-CO_2/year from the atmosphere and delivers a 1.46 Mt-CO_2/year stream of dry CO_2 at 15 MPa. The additional 0.48 Mt-CO_2/year is produced by on-site combustion of natural gas to meet all plant thermal and electrical requirements. Alternate configurations with electricity and gas input are described in the section on Heat and Mass Balance

[1]Harvard School of Engineering and Applied Sciences, 12 Oxford Street, Cambridge, MA 02138, USA

[2]Harvard Kennedy School, 79 John F. Kennedy Street, Cambridge, MA 02138, USA

[3]Carbon Engineering, 37321 Galbraith Road, Squamish, BC V8B 0A2, Canada

[4]Lead Contact

*Correspondence: keith@carbonengineering.com

https://doi.org/10.1016/j.joule.2018.05.006

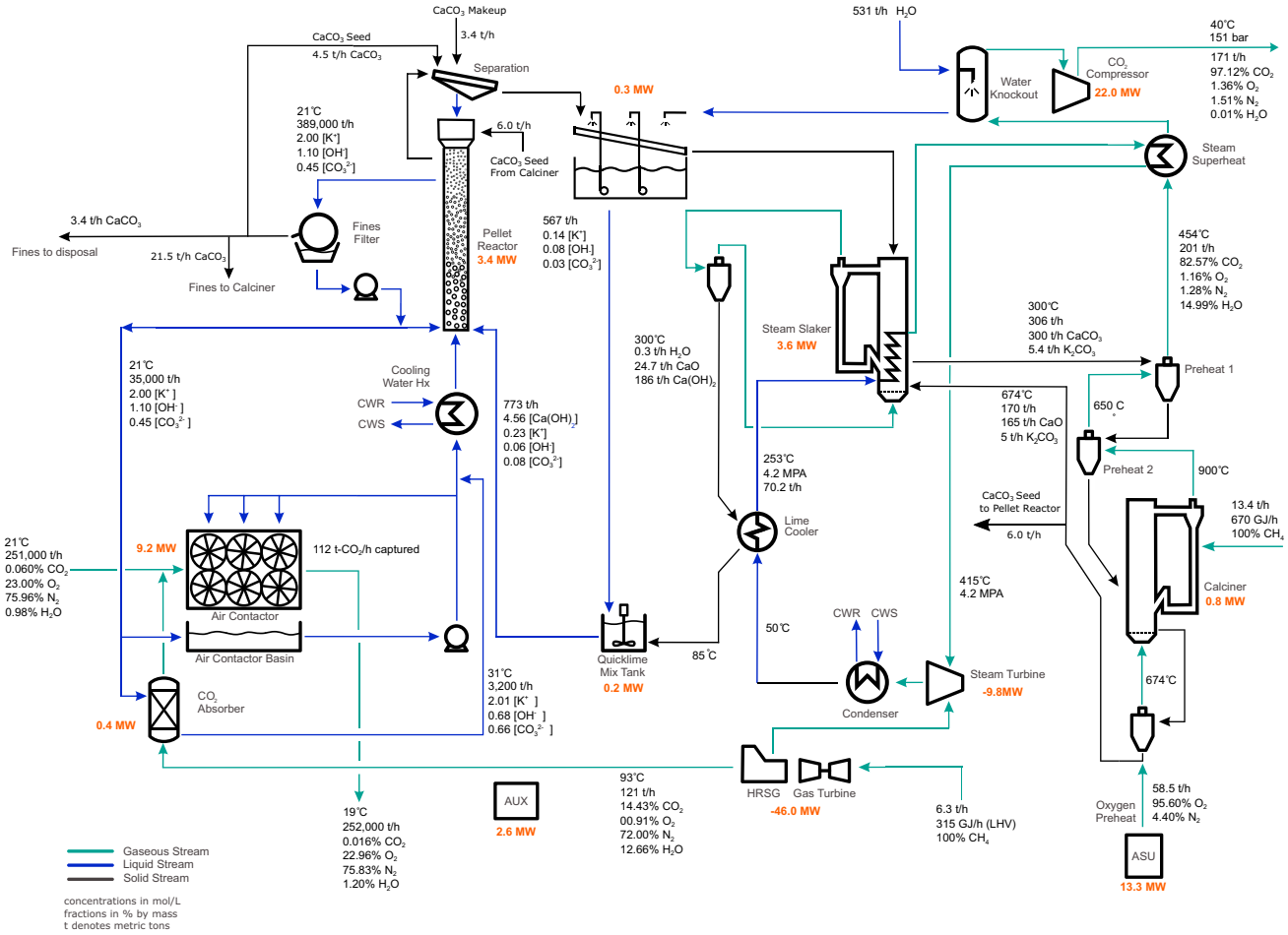

Figure 2. Overview of Process Showing Mass and Energy Balances

Electricity demands are indicated in red as MW. Selected gas and liquid streams show the most important constituents using mass fraction as for gaseous streams and molar concentration for aqueous. Mixed phase streams with substantial solid-phase mass flow are color-coded based on the phase of the gas or liquid transporting the solid. Units are indicated with graphical representations that suggest a schematic physical design of the unit. Many minor streams, such as cooling water to the multistage CO_2 compressor, are not shown. As described in the text, there are several options for introducing the fines stream back into the calciner, these are omitted for simplicity, and this heat and mass balance reflects fines being treated identically to the pellet stream leaving the washer.

and Alternative Configurations and life cycle carbon balance in the section on Avoided Emissions and Life Cycle Accounting.

Energy and material balances come from an Aspen Plus simulation. That simulation depends on performance models of individual unit operations; and these models depend, in turn, on a combination of vendor data and data from the pilot plant described later.

As with any industrial technology, there is a sharp distinction between the ease of developing "paper" designs and the difficulty of developing an operating plant. To paraphrase Rickover: an academic plant is simple, cheap, and uses off-the-shelf components; whereas, a practical plant is complicated, expensive, and "is requiring an immense amount of development on apparently trivial items."[24] CE has now spent roughly 100 person-years on such apparently trivial items to develop a process proposed almost two decades ago by Klaus Lackner and collaborators.[2]

For each unit, we have either identified a vendor of commercial hardware that meets the process specifications or identified commercial hardware that can be adapted to perform the process. In the latter case, we have typically entered into a formal collaboration with a vendor and then tested the unit at a scale the vendor deems necessary to allow specification of commercial-scale hardware. For the major unit operations, this process has involved several cycles of testing at progressively larger scales working with equipment vendors to de-risk the technology. Consider the pellet reactor as an illustrative example of our development process. The idea originated from a paper that suggested use of a Crystalactor[25] developed for wastewater treatment by Royal HaskoningDHV (RHDHV). Working with Procorp Enterprises, RHDHV's American licensee, CE developed a different process configuration.[26,27] The first tests with CE's process conditions were performed in 2011 using Procorp's existing 5-cm-diameter lab unit. CE then contracted with Procorp to build and operate a larger, 30-cm-diameter custom-built system with more appropriate lime injection technology at Procorp's facility in Waukesha, WI. CE then worked with RHDHV and Procorp to design a 1.2-m-diameter system with up to 11 m of fluidized bed depth as part of CE's Squamish pilot plant. Finally, CE built an additional, smaller 14-cm-diameter system at the pilot plant, to speed up testing of alternative operating conditions that are then implemented on the main pilot pellet reactor.

In this section, we first describe the four major unit operations: the contactor, pellet reactor, calciner, and slaker, corresponding to the four reactions depicted in Figure 1. Performance estimates are based on a combination of data from vendors and from our pilot plant (discussed later), along with data from the minor unit operations (see below). These unit performance estimates then drive a chemical process simulation (see below) that provides the values reported in Figure 2.

Contactor

The contactor brings ambient air in contact with the alkali capture solution. Capture of CO_2 from the air occurs at the surface of a ~50 μm film of solution flowing downward through structured plastic packing through which the air flows horizontally (cross-flow configuration). The transport of CO_2 into the fluid is limited by a reaction-diffusion process occurring in the liquid film with a characteristic e-folding length of ~0.3 μm. The mass transfer coefficient for CO_2 (K_L) is most strongly determined by [OH^-] and temperature. We use a semi-empirical formula to estimate the mass transfer coefficient on representative well-wetted structured packings (the "effective" K_L) for a range of fluid compositions and ambient temperatures,[28] which integrates our own empirical data and modeling and aligns with previous literature values.[15,25,29–33] A typical K_L is 1.3 mm/s at 20°C and a typical solution composition of 1.0 M OH^-, 0.5 M CO_3^{2-}, and 2.0 M K^+.

CE's contactor is based on commercial cooling-tower technology, and the design has benefited from close collaboration with SPX Cooling Technologies (SPX), a leading vendor. While the geometry and fluid chemistry differ from conventional cooling towers, CE's design relies on many of the same components, including fans, structured packings, demisters, fluid distribution systems, and fiber-reinforced plastic structural components.

The contactor is the heart of CE's air capture technology. It is the unit that diverges farthest from industrial precedent in that cross-flow cooling-tower components are used for a chemical gas-exchange process, rather than the counterflow vertically oriented tower philosophy typically used for chemical processes. This design choice is a crucial enabler of cost-effective DAC, as designs using vertical packed towers are

Table 1. Summary Data on Major Unit Operations

Parameter	Value	Justification
Contactor		
Process parameters		
Mass transport coefficient	1.3 mm/s	pilot data and laboratory work[28]
Air velocity	1.4 m/s	economic optimization of capital and operating costs[23]
Packing specific surface	210 m^2/m^{-3}	packing parameters are based on Brentwood XF12560 with pressure drop reduced by 30% (see section on the Contactor)
Packing pressure drop	9.7 Pa/m at 1.4 m/s	
Packing air travel depth	7 m	economic optimization of capital and operating costs[23]
Max liquid flow	4.1 L/m^2s	required for full wetting—manufacturer's specification
Average liquid flow	0.6 L/m^2s	pilot data on flow rate cycling
Performance metrics		
Fan energy	61 kWh/t-CO_2	ΔP from pilot data and 70% fan efficiency from SPX
Fluid pumping energy	21 kWh/t-CO_2	pump efficiency 82% from GPSA data book
Fraction of CO_2 captured	74.5%	performance model validated by pilot data
Capture rate unit inlet area	22 t-CO_2 m^{-2}/year	determined from velocity and fraction captured assuming 400 ppm CO_2
Pellet Reactor		
Process parameters		
Fluidization velocity	1.65 cm/s	pilot and benchtop show good performance at 1.65 cm/s for our target pellet size, performance degrades for significantly lower velocities
Bed height	4.5 m	rough optimization of cost of managing fines versus cost of increasing retention; optimization uses empirical performance model driven by pilot data
Calcium loading	20 kg-Ca/m^2hr	
Pellet size	>0.85 mm	pellets removed from bed by passing over a 20 mesh (0.85 mm opening) shaking screen
Performance metrics		
Calcium retention	90%	performance model driven by pilot data
Fluid pumping energy	27 kWh/t-CO_2	determined from loading rate, fluidization velocity, and pumping efficiency of 82% based on GPSA data
Calciner		
Process parameters		
Bed bulk density	710 kg/m^3	pilot data
Fluidization velocity	0.25–2.5 m/s	minimum and operating fluidization velocity from pilot data
Operating temperature	900°C	reaction thermodynamics and pilot data
Performance metrics		
$CaCO_3$ → CaO conversion efficiency	98%	pilot data
Energy consumption	4.05 GJ/t-CO_2	determined by Aspen Plus simulation in consultation with Technip
Slaker		
Process parameters		
Pellet water carryover	11% by mass	pilot data
Operating temperature	300°C	estimate based on preliminary tests
Performance metrics		
Power produced from slaking heat	77 kWh/t-CO_2	estimate from simulation, note that the slaker also consumes 32 kWh/t-CO_2
Conversion to CaO	85%	estimate based on tests conducted by Ben Anthony at CanmetENERGY
Auxiliary Equipment Specifications		
ASU power usage	238 kWh/t-O_2	quote from major ASU vendor for 95% purity delivered at 120 kPa
CO_2 absorber—capture frac	90%	Aspen simulation

(*Continued on next page*)

Table 1. *Continued*

Parameter	Value	Justification
CO_2 absorber—pressure drop	1 kPa	
Compressor power usage	132 kWh/t-CO_2	Aspen simulation, with validation from independent calculations

For each major unit we provide some important process parameters internal to the unit as well as the most important unit performance parameters. Energy consumption values are given for each ton of CO_2 processed by the unit where for calciner, slaker, and compressor, the amount processed is larger than the amount captured from air because of the CO_2 from the power cycle.

far more expensive.[4,14,25] In this paper, we provide only a short overview because the design is described elsewhere.[23] Major differences between our design and common cooling-tower practice include packing depths of ~7 m rather than the ~2–3 m common in cooling towers with structured packing, and use of cyclic-pulsing solution flow to minimize pumping energy while maintaining good packing wetting.[34] The air velocity and packing depth are chosen to minimize combined capital and energy cost,[23] and the resulting design parameters summarized in Table 1.

Working with packing manufacturers and using computational fluid dynamics simulations performed by Professor John Grace's group at the University of British Columbia (UBC), we find that minor changes to packing geometry can significantly reduce pressure drop while retaining similar mass transfer performance. Pressure drop can be reduced by >30% compared with the Brentwood XF12560 packing we used in the pilot for the same air velocity and surface area density. Improvements on established designs are possible because we are optimizing for different conditions: CO_2 uptake differs from the evaporation and sensible heat exchange in a cooling tower, as does our use of pulsed flow to maintain a largely stagnant surface film. Indeed, changes in the tradeoffs between fan energy and capital cost alter the optimal design.[23] Here, we assume that packing in a commercial plant would have a pressure drop 30% lower than XF12560.

Pellet Reactor

Carbonate ion is removed from solution by causticization in the pellet reactor (reaction 2). In this fluidized bed reactor, 0.1–0.9-mm-diameter $CaCO_3$ pellets are suspended in solution that flows upward at ~1.1–2.5 cm/s. A slurry of 30% $Ca(OH)_2$ is injected into the bottom of the reactor vessel (where here and throughout slurry compositions are mass fractions). As Ca^{2+} reacts with CO_3^{2-} it drives dissolution of $Ca(OH)_2$ and precipitation of $CaCO_3$, but the fraction of Ca^{2+} that is precipitated onto pellets depends on maintaining a high surface area of pellets relative to the area of circulating fines while minimizing localized high supersaturations of $CaCO_3$ that form fines. Small seed pellets are added at the top of the bed, and as pellets grow they sink through the reactor until finished pellets are discharged at the bottom. Roughly 10% of the Ca leaves the vessel as fines that must be captured in a downstream filter. The finished pellets are roughly spherical agglomerations of calcite crystals with negligible porosity.

This process is adapted from water treatment technology developed by RHDHV, where it is used to remove multi-valent ions such as CO_3^{2-}. The process was reengineered to allow formation of $CaCO_3$ pellets in high ionic strength solutions. Our process differs from water treatment in that (1) the causticization agent is the limiting reagent, (2) it uses 30% lime slurry rather than the ~2% slurries used in water treatment, and (3) the process parameters are optimized to maximize caustic flux per unit bed area rather than water flux.

As described above and in the section on the Pilot Plant, our process was developed iteratively using several generations of prototypes. The industrial design draws on

RHDHV's experience in engineering and operating large-scale wastewater treatment plants. The high-concentration lime slurry required abandoning the standard dosing racks and adopting a Spiractor configuration,[35] but unlike a free-standing Spiractor vessel, conical feed sections form an egg-carton-like bottom for a large concrete reactors. Similar systems have been used at the Groote Lucht Wastewater Plant and at Bahrain Tubli Wastewater Plants. The Bahrain plant, for example, has a flow rate of 66 m^3/s providing a solid basis for cost estimates on our plant, which has a flow rate of 166 m^3/s.

Our choice of pellet reactor and oxy-fired circulating fluidized bed (CFB) are at the heart of the innovations that reduce the capital and energy cost of the DAC process compared with use of a Kraft caustic recovery loop, which accomplishes the same chemical process in Figure 1. Early process development work at CE and elsewhere considered using the Kraft process followed by a separate CO_2 capture process on the Kraft kiln off-gases as the minimum-risk baseline technology for an aqueous alkaline DAC process.[4,22,36] (Kraft processes use a Na while our process uses a K to improve CO_2 uptake kinetics.) Performance gains come from the ability to make pellets, rather than "lime mud," which is composed of precipitated 10–50-μm-diameter calcite crystals. The pellets are washed and dried easily, removing the need for vacuum filtration, and resulting in pellets that are drier and have lower alkali carryover than lime mud, which in turn allows use of a CFB rather than a rotary kiln. The lack of vacuum filtration and low water carryover reduces energy consumption in the kiln. Moreover, the CFB has lower capital cost than a rotary kiln and it can be oxy-fired.

Calciner

Calcination of $CaCO_3$ to produce CO_2 (reaction 3) is accomplished in an oxygen-fired CFB. Our design has been developed in collaboration with Technip's Dorr-Oliver Fluosolids Systems Division from initial design through laboratory testing, CE's pilot plant, and design of the commercial-scale calciner. Technip has deployed high-temperature fluidized beds at comparable scales, including, for example, two 6.7-m-diameter oxygen-blown CFBs used as gold ore roasters in the Goldstrike mine in Nevada.

The calciner, along with preheat cyclones, are large steel vessels lined internally with refractory brick. Fluidizing gas is supplied into the bottom of the calciner through a distribution plate made from an arch of refractory, and natural gas is injected directly into the fluidized bed just above the distribution plate using a series of lances.

Our conservative heat integration design reduces technical risk compared with alternate designs that maximize energy efficiency at the expense of higher capital cost and technical risk. Incoming pellets, which arrive from the steam slaker at 300°C, pass through two heat recovery cyclones arranged in counter-current configuration with the outgoing gas stream. In the first preheat cyclone, the incoming solids are preheated to 450°C by cooling the outgoing gases from 650°C to 450°C. In the second preheat stage, the solids are further heated to 650°C by cooling the gases from 900°C to 650°C. Following the cyclones, the outgoing gas stream drives a steam superheater, further cooling the gases to 325°C and producing steam for power generation. The outgoing CaO from the calciner is cooled to 674°C in a single cyclone, which in turn preheats the incoming oxygen to the same temperature before the CaO is sent to the steam slaker.

The calciner operates at ambient pressure. Leakage of nitrogen into the system is minimized by using steam-fluidized loop seals at the inlet to the steam slaker and

between the steam slaker and the calciner. Experience with similar dual fluidized bed systems with intermediate loop seals[37] suggest that in a worst-case scenario, the steam slaker atmosphere would contain 0.4% air contributing 0.0013% N_2 (by volume) to the calciner off-gases.

As our process is, in some respects, derived from the Kraft pulp process, it is useful to compare this calciner with the rotary kilns used in the Kraft process. A single 6-m-diameter CFB of this design will have a capacity of 2 kt-CaO/day. A typical large Andritz rotary kiln calcining lime mud is 5.5 m diameter × 165 m long and produces 1.6 kt-CaO/day.

Process parameters are summarized in Table 1. The minimum required energy to drive the reaction is 3.18 GJ/t-CaO. Our design requires 4.07 GJ/t-CaO equivalent to 5.25 GJ/t-CO_2 (that is, CO_2 from calcination) to make up for thermal inefficiencies in heating the feed streams and heat losses to ambient air. This makes the calciner approximately 78% thermally efficient, substantially higher than lime mud calciners, which have thermal efficiencies of roughly 39%, though less efficient than limestone calciners, such as the Cimprogetti TWIN-D shaft kilns, which are 89% efficient on the same basis. Our calciner choice and its efficiency are enabled because pellets are easy to dewater and have appropriate fluidization properties.

Steam Slaker

Heat from slaking (reaction 4) is used to dry and preheat the pellets, yielding sufficient steam to sustain the slaking reaction.[33] The thermodynamic advantage of steam slaking over conventional water slaking used in the Kraft process is that the slaking reaction enthalpy is released at higher temperatures. Maximum temperature is 520°C for slaking in 100-kPa steam, whereas we operate at 300°C to achieve fast kinetics.

Designed in partnership with Technip, the slaker is a refractory lined bubbling/turbulent fluid bed that is fluidized by recirculating steam flow.[38] It receives ambient temperature $CaCO_3$ pellets from washing and hot CaO at 674°C from the calciner's oxygen preheat cyclone. Fluidization velocity is 1 m/s, which transports and slakes quicklime (CaO) particles to form $Ca(OH)_2$. Small quicklime particles are elutriated and recirculated by a primary cyclone and loop seal, while the much finer slaked particles mostly bypass the cyclone and are captured in a dust collector. The outgoing stream is 300°C hydrated lime, from which sensible heat is recovered and, along with heat from the slaking reaction, used to dry and warm the pellets. Dry 300°C pellets are then fed into a closed-loop pneumatic conveyor driven by recirculating CO_2 and steam to deliver them to the top of the calciner stack.

Minor Unit Operations

Beyond the four major units described above, the plant requires many additional unit operations that are "minor" in the sense that they present little or no technical risk. This section summarizes configuration of the power island along with the absorber that captures CO_2 generated from power production, the CO_2 compression and cleanup, and the oxygen plant. Key performance characteristics for each of these units are provided in Table 1.

Power Island. The power island consists of a natural gas turbine, followed by a heat recovery steam generator (HRSG). We model a GE LM 2500 DLE with a 2 × 1 HRSG configuration. The resulting steam is combined with steam from the slaker, passed through the superheater (to extract heat from the calciner off-gases), and then

Table 2. Summary Performance of Various Plant Configurations

Scenario	Gas Input[a] (GJ/t-CO_2)	Electricity Input[a] (kWh/t-CO_2)	C-Gas/C-Air	Capital $ per t-CO_2/year	O&M[b] ($/t-$CO_2$)	Levelized[a] ($/t-$CO_2$)	
						CRF[c]	
						7.5%	12.5%
A: Baseline: gas fired → 15 MPa CO_2 output	8.81	0	0.48	1,146	42	168	232
B: Baseline with N^{th} plant financials	8.81	0	0.48	793	30	126	170
C: Gas and electricity input → 15 MPa CO_2 output	5.25	366	0.30	694	26	113–124	152–163
D: Gas and electricity input → 0.1 MPa CO_2 output assuming zero cost O_2	5.25	77	0.30	609	23	94–97	128–130

[a]Gas and electrical inputs as well as levelized cost are all per ton CO_2 capture from the atmosphere.
[b]Non-energy O&M expressed as fixed per unit of capacity with variable costs including cost of make-up streams included and converted equivalent fixed costs using 90% utilization.
[c]CRF is the average capital recovery factor defined in the section on Process Economics. Calculations assume NG at 3.5 $/GJ and a 90% utilization. For the C and D variants levelized costs are shown as a range using electricity at 30 and 60 $/MWhr.

used to drive a steam turbine that generates the remainder of the power required by the plant. To reduce complexity, our Aspen simulation approximates this using independent steam cycles for the gas turbine and slaker/superheater. After heat recovery, gas turbine exhaust is sent to the CO_2 absorber.

CO_2 Absorber. The gas turbine exhaust stream is stripped of CO_2 using a conventional counterflow gas-liquid column, using a portion of the fluid stream returning from the contactor. Based on rough optimization using Aspen, we chose a 12 × 7.5 m (height × diameter) column filled with 95 m^2/m^3 BERL Ceramic packing that captures ~90% of inlet CO_2 with a pressure drop of 1.08 kPa at an average operating gas velocity of 0.75 m/s. The absorber outlet is ducted to main air contactor where ~75% of the remaining CO_2 is captured.

CO_2 Compression and Cleanup. Compression is accomplished using a standard centrifugal compressor. Performance and power demand were simulated on a four-stage centrifugal compressor based on Dresser-Rand data, with a glycol system for dehydration prior to the final stage, and going from atmospheric to 15 MPa at 45°C. The compressor cost estimate included inter-stage coolers and scrubbers, and cost of equipment was generated by Aspen's Capital Cost Estimator and compared with previous vendor estimates.

Oxygen Plant. We use a conventional cryogenic air separation unit (ASU). Large ASUs are available in multi-train complexes that produce over 30 kt-O_2/day. Cryogenic ASUs typically produce oxygen up to 99.8% purity and 10 MPa. Cost was estimated by Solaris (see the section on Process Economics) based on a vendor quote for a 1.5 kt-O_2/day system. Power demand of 238 kWh/t-O_2 for a 120 kPa delivery pressure was estimated by a major ASU vendor.

Heat and Mass Balance and Alternative Configurations

The plant's simplified heat, mass, and power balance are shown Figure 2, with energy inputs summarized in Table 2. At ambient conditions of 20°C and 64% relative humidity, the plant needs 4.7 tons of water per ton CO_2 captured from the atmosphere. This ratio varies with ambient conditions and solution molarity; this relationship is shown in Figure 3F, which was calculated with Aspen data and validated with CE's pilot air contactors. The plant discharges 1% of the circulating Ca each cycle as waste, this discharge serves as a purge that manages the buildup of non-process elements that

enter the cycle by various routes, most importantly as dust ingested into the contactor. At this discharge rate, CE estimates that Ca disposal and make-up contribute a cost of \$0.22/ton-CO_2 to the overall totals presented in this paper.

Process Simulation. Plant performance was computed in Aspen Plus V8.0. We use the ENTRTL-RK and RK-SOAVE thermodynamic property packages for aqueous phase and gaseous phase respectively. We used the following APV732 property databanks: ASPENPCD, AQUEOUS, SOLIDS, INORGANIC, and PURE26. Gas solubility and the precipitation of salts were specified manually. Chemical loops were converged in Aspen's sequential modular mode. Many individual unit parameters, including much of the data from Table 1 are computed in a set of linked external spreadsheets.

Scaling. The performance of any large industrial process depends on scale. Both the air contactor and the pellet reactor are modular, so their performance varies little from 1 Mt-CO_2/year down to sizes as small as 10 kt-CO_2/year, and their capital cost per unit capacity is nearly constant down to 100 kt-CO_2/year. In contrast, the calciner is a large refractory lined vessel with complex equipment for thermal integration, which results in both performance and cost scaling strongly with size. This calciner design is appropriate down to an internal diameter of about 1 m corresponding to a capture rate of 15 kt-CO_2/year, but CE judges that—given cost scaling—the smallest economically practical size for the complete process is about 100 kt-CO_2/year. At that scale, for the full DAC process, the energy intensity would very close to the 1 Mt-CO_2/year baseline, but the capital cost per unit of capacity would be ~80% larger.

Alternative Configurations. CE is developing various plant configurations to address specific markets. These configurations all share the four core unit operations described above, but vary in their treatment of power system, oxygen supply, and CO_2 compression.

The baseline plant configuration, "A" on Table 2, is applicable to geologic storage in locations with comparatively low natural gas prices, so this scenario delivers CO_2 at specifications appropriate for pipelines. While actual plants will be grid connected, for convenient analysis we have sized the power system in this baseline configuration so that the facility is electrically neutral with no net power input or output.

An N^{th} plant variant with the same configuration, "B," is included to reflect improvement in capital and construction costs that vendors and engineering, procurement, and construction (EPC) firms have indicated would be realized following early plant builds as we improve constructability and build supply chain relationships.

We also report two additional process variations upon the baseline. A variant with minimum gas input, "C," has no gas turbine and uses grid electricity to make up all power not supplied by the steam cycle running off the steam slaker. Overall cost and energy requirements are summarized in Table 2. Note that this variant requires a few minor process alterations not shown in Figure 2. This variant is appropriate for locations with low-carbon-intensity low-cost power.

Finally, variant "D" is optimized to provide CO_2 for fuel synthesis. CE is developing air-to-fuel systems in which the hydrogen required as feedstock for the fuel synthesis step is produced by electrolysis.[39] In this configuration, the oxygen from electrolysis is sufficient to supply the DAC plant, so in this application we drop the ASU from the DAC process. The fuel synthesis system requires a CO_2 supply pressure of ~3 MPa, reducing the cost and complexity of the CO_2 compression and clean up. CE is

developing methods to integrate the DAC and fuel synthesis, but for simplicity of analysis, here we show (Table 2) the inputs for a plant that receives O_2 and produces atmospheric pressure CO_2.

Pilot Plant

The design or operating conditions of several of the important unit operations in our process differ sufficiently from their industrial counterparts, and as such require process optimization and testing. To address this need as well as the overall integration risk, CE has operated a pilot plant on a 0.5-hectare industrial site in Squamish, BC, since 2015.

The design goal for the pilot were (1) to test each unit operation for which there is significant technical risk at a scale the equipment supplier judged sufficient to allow specification of commercial-scale hardware, and (2) to test the most important units as components of a closed-loop process. The pilot plant builds on previous prototype data that CE acquired for each unit, and on work with SPX, RHDHV, and Technip to design and size the contactor, pellet reactor, and calciner, respectively. CE's pilot data have been used to refine the commercial-scale plant design described earlier.

The pilot is not a complete small-scale version of a commercial plant, as units that were judged low risk are not included. For example, the pilot does not include gas clean up and CO_2 compression downstream of the calciner, as these processes present minimal technical risk. The air contactor and pellet reactor operate as a coupled loop with a capacity of 0.6 t/day of CO_2 captured from the air, a scale at which each unit is large enough for validation of commercial-scale hardware. The minimum scale for the calciner corresponded to roughly double this capacity, so while the contactor, pellet reactor, and slaker can operate continuously, the pellets are accumulated in a storage silo and then the calciner is run in batch mode to process the accumulated pellets and produce lime. Finally, the slaker was chosen to close the overall chemical loop and to produce lime slurry in a stirred tank reactor, rather than in a steam slaker, as discussed earlier.

Pilot Contactor

The pilot contactor tests the performance of CE's cooling-tower-derived packing, drift elimination, and fluid distribution systems. The structure is modified from an SPX commercial unit in which air flows inward through two banks of structured packing and enters a central plenum where it is ejected upward through a vertical-axis fan. Each packing bank has a 3 × 5-m inlet cross section with a 3-m depth of Brentwood XF12560 structured packing. (This depth, although sufficient for pilot testing, is smaller than in the full-scale air contactor design, and thus the pilot capture fraction is lower than at commercial scale.) Standard SPX construction and fluid distribution techniques are used, including extensive use of low-cost fiberglass-reinforced plastic. While the overall geometry differs slightly from CE's single-bank commercial design, the pilot tests the packing and distribution systems as well as the construction methods and materials choices at scales that imply minimal further scale-up risk given the inherently modular nature of the full-scale design.[23] At an inlet velocity of 1.4 m/s the contactor ingests air at 180 t/hr, yielding a 45 kg-CO_2/hr maximum capture rate at 42% capture fraction.

Figure 3 shows selected pilot plant air contactor data, and Figure S2 shows images of CE's pilot air contactor and industrial analogs. Pressure drop closely matches specified performance (Figure 3A) and is stable over ~0.75 year, demonstrating minimal long-duration fouling. Pressure drop increases with liquid flow rate as seen in Figures 3B and 3D, and the sequence of small flow pulses is designed to reduce fluid and air pumping energy. Large pulses are used occasionally to flood the packing, ensuring

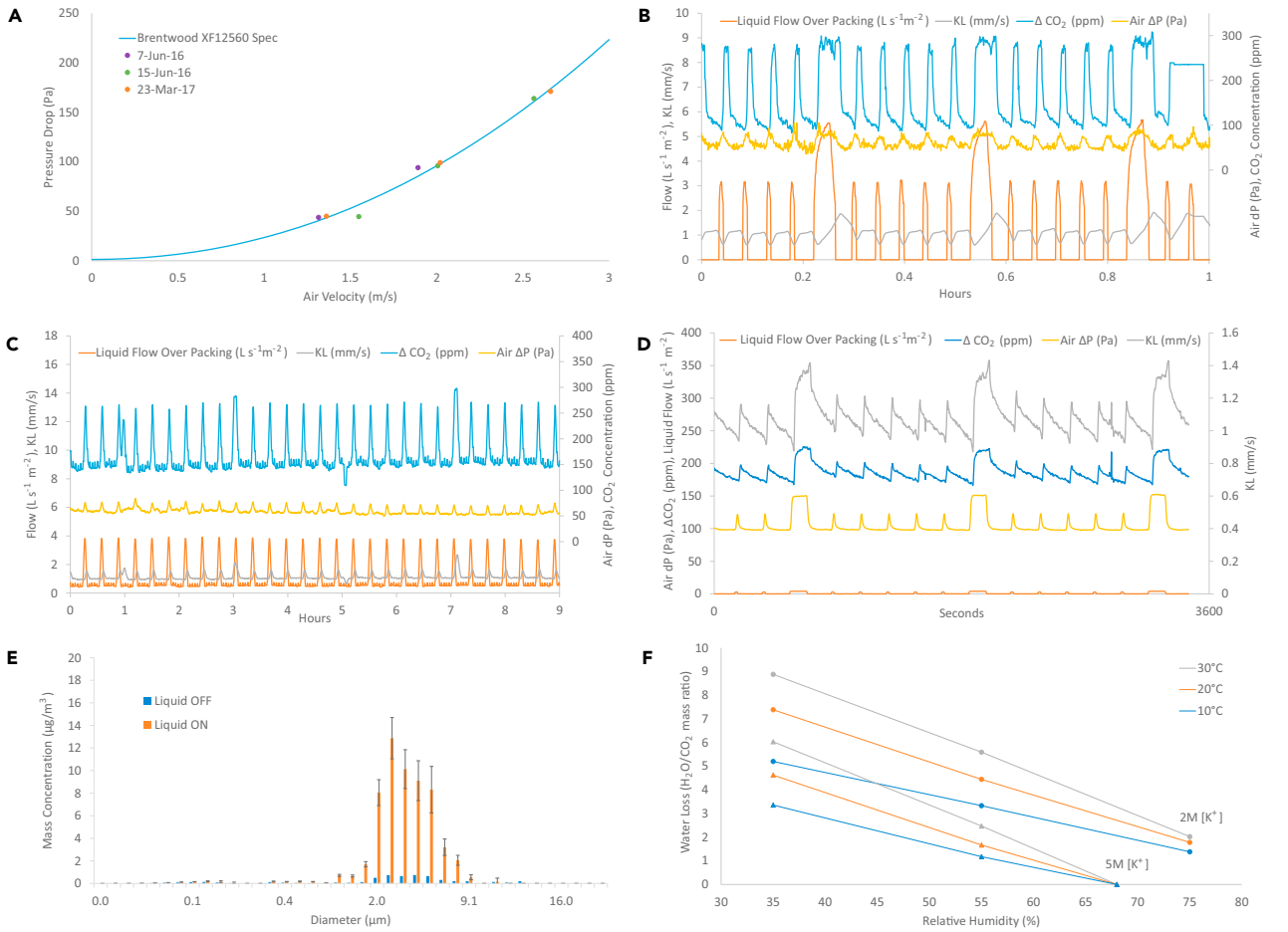

Figure 3. Selected Data from Pilot Contactors

(A) Pressure drop through dry packing and drift eliminator.

(B) Time series pilot contactor operation showing alternation of large and small packing fluid refresh cycles, data are from July 2016 with average air flow velocity of 1.17 m/s at 18 C ambient temperature.

(C) Eight hours of data showing same variables with same color key as in (B).

(D) Time series from a prior CE contactor pilot in 2012 at average air flow velocity of 1.45 m/s showing similar cycling at using a 2.6 M [OH^-] solution.

(E) Particle size distribution measured at contactor outflow showing contrast between drift with liquid flow on and off. Values are total mass per unit volume in size bins with centers indicated on the x axis, and error bars are standard deviation across five measurements.

(F) Calculated water loss from evaporation in the air contactor as a function of temperature, relative humidity, and total capture solution molarity.

complete wetting. Using observed air velocity and fraction of CO_2 removed, along with packing depth and surface area density, we use equation 2.1 of Holmes and Keith[23] to derive an "effective" mass transfer coefficient, $K_{L\text{-eff}}$, that is the product of K_L and the surface wetting efficiency. Pressure drop, mass transfer, and drift measurements are all consistent with 2012 results from a previous prototype air contactor[40] and from laboratory data.[28] Note that due to challenges of getting an accurate spatial average of ΔCO_2 measurements across the contactor outflow, we use data from a representative location scaled to match the time-integrated changes in liquid chemistry that provide the most accurate long-term uptake measure.

One potential risk of using cross-flow cooling-tower components is that droplets of contactor fluid can escape into the ambient air, posing a health hazard. The cooling-tower

industry calls such fluid loss "drift." CE has measured total drift concentrations using standard air quality monitoring vacuum filters followed by quantitative measurement of the alkali content of the filter paper. In addition, we collaborated with Professor Steven Rogak's group at UBC. They used a TSI NanoScan SMPS optical particle sizer and aerodynamic particle sizing instruments to produce the size distribution data shown Figure 3E. All measurement techniques have shown airborne KOH concentrations less than 0.6 mg m^{-3} of air at contactor outflow, which is well below the 2.0-mg m^{-3} National Institute for Occupational Safety and Health (NIOSH) ceiling recommended exposure limit.[41] This drift performance is consistent with specified performance for the Marley XCEL TU cellular drift eliminator used in our design.

Performance depends on ambient conditions. Water loss is determined by ambient temperature, relative humidity, and molarity of the capture solution (Figure 3F). K_L is affected by temperature but not significantly by humidity.[23] Fluctuations in K_L caused by diurnal or seasonal temperature changes are material and can be partially compensated for by adjusting the gas and liquid throughputs.

Pilot Pellet Reactor

Our pilot is a steel vessel with internal height of 12 m, a 1.2-m diameter, and a 60° conical base, similar to a single cell of the commercial design. Ancillary equipment allows automated addition of seeds, extraction and processing of fines, and washing/drying of mature pellets. It was designed in collaboration with RHDHV based on a numerical model and on results from tests in 5- and 30-cm-diameter systems by Procorp.

Figure 4 shows selected pilot plant pellet reactor data, and Figure S3 shows images of CE's pilot pellet reactor and industrial analogs. The initial growth of a mature bed from seeds takes several months under typical process conditions (Figure 4D), and the cycle from pellet discharge and seed addition to recovery of the bed density profile is about 2 days (Figure 4A). In addition to the primary pilot, we built two 0.1 × 5.2-m "benchtop" pellet reactors,[18] to allow testing under a larger number of process conditions and to test in conditions that might cause bed collapse and reactor plugging, which would have been difficult to manage in the primary pilot.

Reactor performance depends on bed height, Ca loading rate, fluidization velocity, pellet size at bed base, and the circulating concentration of fine calcite particles (<50 μm) that provide nucleation points for calcite precipitation. Our overall objective is to minimize the energy and capital cost of the reactor while maintaining a retention rate above ~85%, where retention rate is the fraction of injected Ca that leaves the bed as pellets rather than being lost as fines. The pumping energy per unit of Ca flux is proportional to the fluidization velocity and bed height and inversely proportional to the Ca loading rate.

Figure 4B illustrates the impact of fines processing on retention, and much of the design optimization amounts to adjusting other parameters to balance minimizing fines production with minimizing energy cost.

Our initial design assumed a benefit to extending the bed height over 10 m and relied on loading rates of over 40 kg-Ca m^{-2}/hr to get acceptable energy performance. However, we found no increase in retention for bed heights greater than 4.5 m, probably because dissolution-precipitation kinetics were faster than anticipated in the numerical model. Our current design point is a 20 kg-Ca m^{-2}/hr loading rate with a 4.5-m bed height (Table 1). We anticipate small but significant

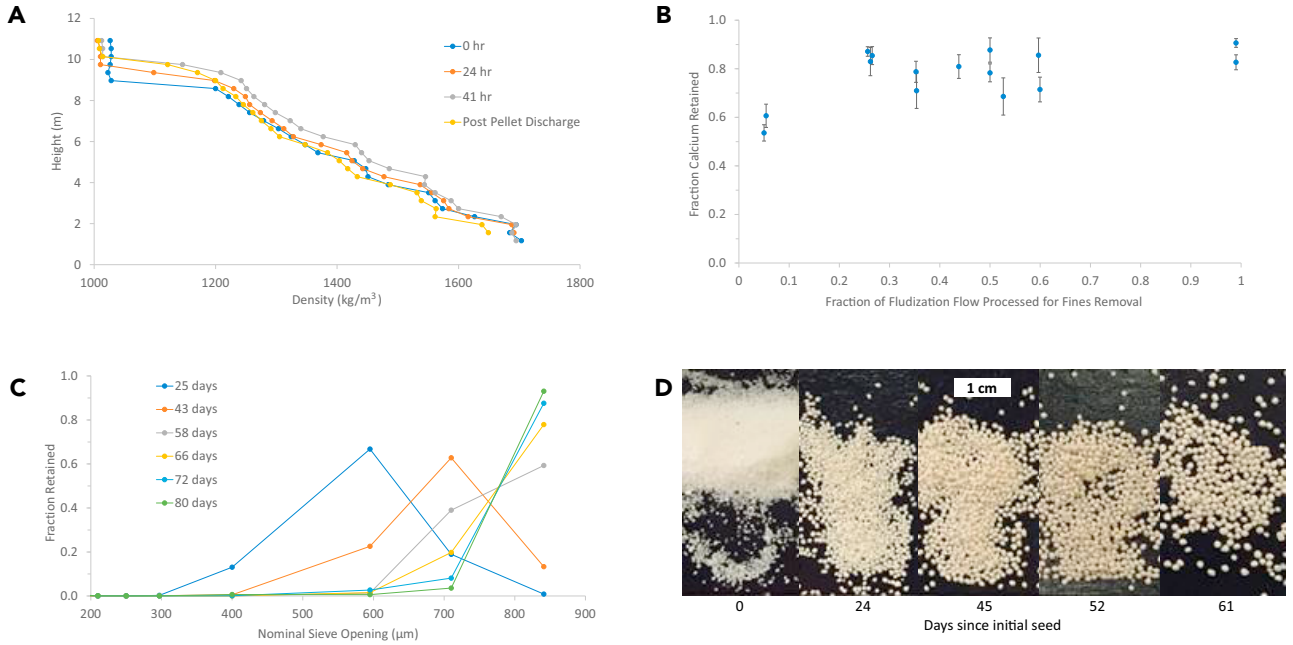

Figure 4. Selected Data from Pilot Pellet Reactors

(A) Pellet reactor density profile during operation and post pellet discharge. Density of slurry at each point within the reactor determined using the apparent immersed weight of an object of known weight and volume.

(B) Calculated calcium retention as a function of the fraction of recirculating flow processed to remove inert "fines" (calcium carbonate) in the benchtop pellet reactor.

(C) Size distribution of sample from bottom of pellet reactor during bed development. Time evolution in days, to show growth of seed material to mature pellet bed measured by passage through calibrated filter screens.

(D) Photos illustrating time evolution of $CaCO_3$ pellets sampled from bottom of pellet reactor bed.

improvements in energy trade-off between energy requirement and retention as we continue to adjust process parameters.

Pilot Calciner

The pilot calciner was designed in close collaboration with Technip following their common practice, which uses data from a specially designed 0.15-m interior-diameter calciner to provide accurate performance predictions for a commercial-scale system. Technip's design uses a steel vessel with an externally heated jacket that effectively eliminates heat loss through the vessel walls and allows the small high surface-to-volume ratio testbed to mimic the bed behavior and in-bed heat transport that would be present in a large refractory lined commercial-scale calciner. Jacket heating is accomplished with a gas-fired external heater and additional electric heaters to manage cold spots.

Hazen Research (Golden, CO) did initial high-temperature testing of CE's pellets, and then CE worked with Hazen, and BC Research Inc. (Richmond, BC) to design, procure, and commission the calciner to meet Technip's test specifications. The pilot is an oxy-fired circulating fluid bed calciner with an 8.5-m-tall riser. It differs from the commercial configuration in that it uses a fluoseal for solids recirculation but not for solids discharge, does not include preheat for the pellets or oxygen, and uses an air quench and baghouse prior to venting to manage off-gases.

The important performance goal was to achieve a high material flux and high calcination, in conditions where reaction enthalpy is driven by in-bed combustion using

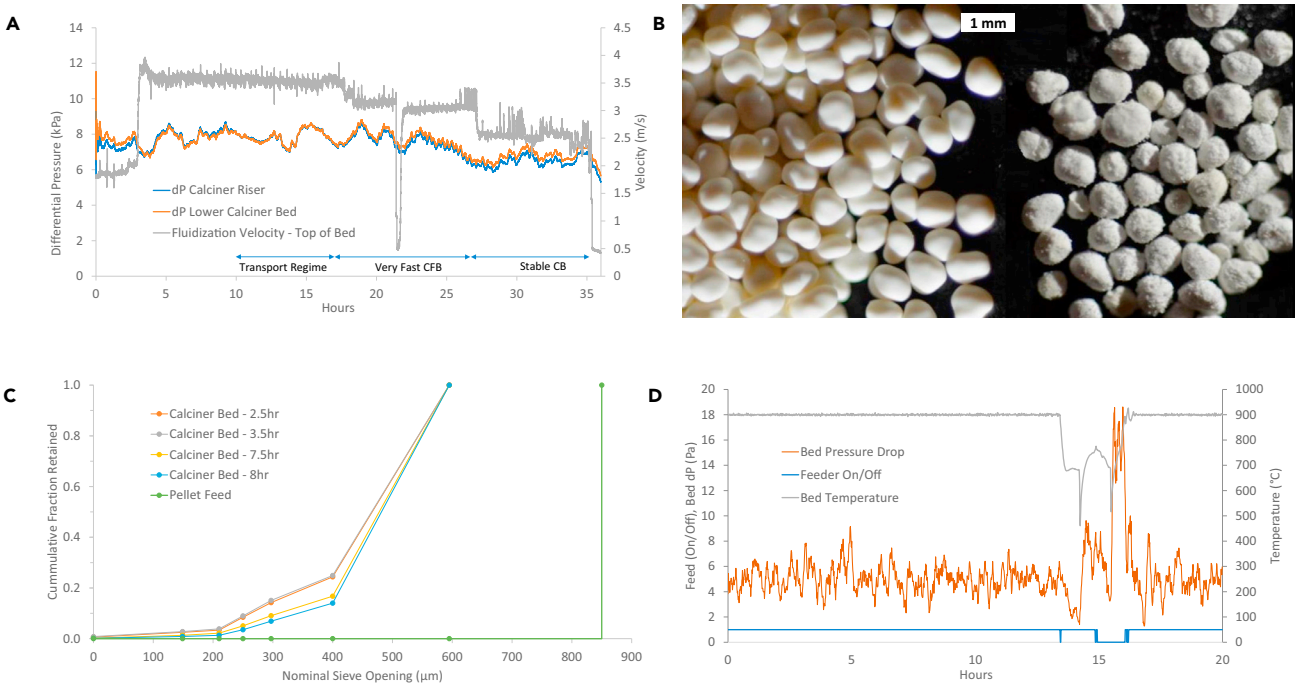

Figure 5. Selected Data from Pilot Calciner

(A) Gas as velocity at bed top computed from flow rates along with pressure drop across two sections of calciner riser. Fluidization regimes as diagnosed from the pressure difference and bed stability at various flow velocities as are indicated.

(B) Photo showing $CaCO_3$ pellets as they are fed into the calciner and CaO pellets at discharge.

(C) Size distribution of bed sampled bed material and feed pellets are measured by passage through calibrated filter screens.

(D) Measured bed temperature and pressure drop for a selected 20-hr duration, showing an upset, and recovery to equilibrium operation, at hr 14 due to an operator error, which led to auxiliary equipment shutting down.

oxygen and natural gas as the sole fluidizing gas. Reaction conversion >98% was measured using chemical analysis and X-ray diffraction analysis on discharged pellets.

Figure 5 shows selected pilot plant calciner data, and Figure S4 shows images of CE's pilot calciner and industrial analogs. We attained the specified 90 kg-$CaCO_3$/hr feed rate over hundreds of hours of run time with stable bed performance, and with stable combustion with excess oxygen concentration of 20%. Note that given the small bed diameter, we did not expect to obtain stable combustion at lower excess oxygen. Based on performance of their commercial oxy-fired calciners, Technip does not expect difficulty achieving the design ratio in a commercial-scale calciner. Throughput is determined by fluidization velocity in the circulating bed regime. Figure 5A demonstrates the reactor's transition from the transport regime (minimal pressure drop) to a stable circulating bed with a 6.5 kPa pressure drop as fluidization velocity is reduced. Feed and product pellets are shown Figure 5B. The fluidization characteristics are, in turn, determined by the particle size distributions shown in Figure 5C.

Another important goal was to determine that rates of fouling—the deposition of materials on interior surfaces of the calciner—were acceptably low for commercial operation. Two kinds of fouling are relevant. Re-carbonization fouling occurs if temperature drops below the re-carbonation temperature allowing CaO and CO_2 to form $CaCO_3$, which forms a hard deposit on surfaces. Alkali fouling is driven by

the sticky alkali species, particularly influenced by carryover of K from the aqueous process. Alkali fouling was judged to pose significant process risk and was an important objective for the pilot. While re-carbonation fouling posed challenges to achieving stable operation of the pilot, Technip anticipates minimal re-carbonation in a larger refractory lined commercial system for which precise temperature control is easier than in our small high-aspect ratio pilot. Once sufficient temperature control was achieved to minimize re-carbonation fouling, the pilot was operated for 90 hr of near-continuous high-temperature operation and minimal alkali fouling was observed, providing confidence to proceed to a commercial-scale calciner.

Process Economics

The cost of new technologies is inherently uncertain. While technology developers may have the most relevant knowledge, they may also have incentives to underestimate costs. In considering the cost of DAC, it is useful to distinguish between adsorption-based technologies[20,42] that typically require manufacture of hardware not yet available in a competitive market at a relevant price, and technologies such as the process described here that requires construction of an industrial facility that will perform a novel process, but that is constructed using commodity equipment and methods. Uncertainties in the first case arise from scaling up a manufacturing process for a new product (the absorber) system, while the uncertainties in the second arise from estimating project construction costs for a new facility. In both cases, additional uncertainty comes in estimating the performance (e.g., capture rate) and from the cost of energy inputs.

Capital Cost

CE uses the structured front end loading (FEL) process[43] for project management. CE has begun development of FEL-3 engineering for a commercial validation plant with a CO_2 capture capacity of order 2 kt-CO_2/year. The project engineering and costing for the 1 Mt-CO_2/year plant described here is FEL-1.

CE's cost estimating process starts with vendors of the major nonstandard unit operations: air contactor, pellet reactor, and calciner/steam-slaker. SPX, RHDHV, and Technip have each worked with CE through years of development, and each have provided budgetary estimates for commercial equipment. The character of these estimates varies with the business model of the vendor. SPX, for example, generally provides firm quotes for the erection of a complete cooling tower on a site prepared by the customer, whereas Technip and RHDHV provide detailed engineering and a limited amount of unique equipment and then work with the customer's EPC firm to oversee construction and commissioning.

All other components are common industrial process equipment available from multiple vendors. Cost estimates for these components start with rough estimates using consultants, equipment vendors, and standard engineering reference sources. CE's engineering group then uses simple multiplicative cost estimating factors to go from equipment costs to estimates of total plant cost.

As a complement to these bottom-up in-house estimates, CE engaged Solaris MCI (Surrey, BC, Canada), a midsized EPC firm, to provide a substantially independent project cost estimate. Solaris worked with major vendors and used their proprietary cost database and factorial project cost estimating methods. The Solaris scope included civil works and utilities. The resulting capital cost and summary justifications are provided in Table 3. In our estimates, we define equipment cost (EC) as major purchased equipment, Materials cost (MC) as materials such as cement and

Table 3. Capital Costs, Given in $M USD (in 2016 Dollars)

Module	Early Plant EC	Early Plant MC	Early Plant LC	Early Plant TDFC	Nth TDFC	Justification
Air contactor	$114.2	$48.0	$50.0	$212.2	$132.8	SPX provided an estimate for DAC air contactors designed in conjunction with CE. Scope includes contactor structure, top and bottom basins, all liquid piping, fans, gear-reducer, and fan motors. SPX estimate includes field installation. This estimate includes civil work, concrete foundations, liquid pumps and supporting utilities, piping, and instrumentation and controls. Solaris then used estimating tools to provide final EC, MC, and LC roll ups
Pellet reactor	$76.9	$28.4	$25.5	$130.7	$94.8	quote from DHV was for major equipment, material, and labor but did not include design, engineering management, and permitting. Solaris then estimated equipment costs at 60% of the RHDHV estimate and broke down the equipment costs into components in DHV quote. Solaris then used ACCE to build up TDFC. Working backward from the ACCE output, 60% of the TDFC is within 1.5% of the original 60% estimate in RHDHV quote
Calciner-slaker	$43.8	$18.1	$15.8	$77.7	$63.6	Technip provided a budgetary cost estimate for the steam slaker and calciner equipment which totaled $16-20 M. Using typical scaling factors based on their project experience installing this type of equipment, they estimated that the TDFC should be between $70 and $90 M. Solaris used this information as the basis of their costing analysis in ACCE. The number of calciner/steam slaker units (40 and 12, respectively) was adjusted so the TDFC output from ACCE landed within the $70-90 M estimate from Technip
Air separation unit	$38.0	$0.0	$16.3	$54.3	$46.7	based on quoted data to Solaris for similar ASU projects. Cost source from vendor budget quote for a 1,500 t/day O_2 unit (95%) purity. Labor estimated at 250,000 hr from Solaris in-house experience. Nth plant has a 20% reduction in material cost with the same labor hours
CO_2 compressor	$17.2	$1.4	$1.4	$19.9	$15.5	assumed to be a multistage centrifugal compressor; four stages, inter-stage coolers and scrubbers included. Sizing data estimated based on HYSYS simulation for compression of CO_2, and Solaris internal database
Steam turbine	$6.7	$0.4	$0.4	$7.51	$5.8	cost of equipment was generated by ACCE based on CE-required specs and compared against available vendor budgetary quotes and in-house data from similar facilities
Power plant	$32.7	$0.9	$1.4	$35.03	$26.7	cost of equipment was generated by ACCE based on CE-required specifications and compared against available vendor budgetary quotes and in-house data from similar facilities
Fines filter	$17.6	$7.1	$6.2	$30.9	$24.8	CE commissioned Procorp to perform a filtration costing study based on CE's process conditions, which produced the estimated equipment cost. The equipment cost used similar ratios of EC, MC, and LC to TDFC to develop a TDFC
Other equipment	$96.9	$3.4	$2.5	$102.9	$77.0	assumed to be 20% of the cost for the rest of the process equipment, including the CO_2 absorber for the power cycle. Auxiliary equipment was input as a quoted item where only the cost of material could be specified; 20% assumption was made to include the ancillary equipment for which no data on design basis was available to Solaris. Pipe rack cost was generated by ACCE
Buildings	$2.5	$0.0	$4.2	$6.7	$5.8	cost of equipment/area generated by ACCE. Building dimensions estimated from plot plan
Transformer	$ -	$18.6	$1.2	$19.8	$16.7	assuming 75,000 kVa rated load at 25 kV. Cost from ACCE based on CE-required specs and validated by Solaris against vendor budgetary quotes
Total direct field costs				$697.7	$510.1	
Indirect field costs				$88.5	$68.8	Solaris estimate including field construction supervision, start-up, and commissioning
Total field costs				**$786.2**	**$578.9**	
Engineering				$135.2	$78.0	assumed to be 12% of TPC less engineering for early plants, 10% of TPC less engineering for N^{th} plant
Other project costs				$48.2	$35.8	Solaris estimated charges for home office, G&A, and contract fee
Contingency				$157.2	$86.8	assumed to be 20% of total field costs for early plant, and 15% for N^{th}
Total non-field costs				$340.6	$200.6	
Total project costs				**$1,126.8**	**$779.5**	

Estimated capital costs are for a plant design shown in Figure 2 that has a capacity of 0.98 Mt-CO_2/year from the air. Annual quantity captured is lower given utilization. ACCE, Aspen Capital Cost Estimator.

piping not included in EC, and labor cost (LC) as on-site construction labor. Total direct field costs (TDFC) are the sum of EC, MC, and LC. Indirect field costs (IFC) comprise material and labor for construction along with benefits, burdens, consumables, insurance, and other miscellaneous costs. Non-field costs (NFC) comprise engineering, contingency, other project costs such as home office, general and administrative, contract fees, and taxes. Total project cost (TPC) is the sum of TDFC, IFC, and NFC.

Contingency allowances on large projects account for three risk categories: project, strategic, and contextual. Project risks comprise equipment and supply chain risks along with all site-related risks. Strategic risks account for business issues such as joint venture negotiations, changes to the project objectives, or resource management. Contextual risks are those resulting from dependence on current laws, geopolitics, and economic conditions. We account for project risks by adding 20% of TDFC and IFC for the early and plant configuration and 15% for N^{th}, but we excluded strategic and contextual allowances. Note that the 20% project contingency used here is too low for a first of a kind plant.[44] CE anticipates that its first plants will be smaller than that the 1 Mt-CO_2/year analyzed here. Our "early plant" value assumes risks have been reduced by construction of a sub-scale commercial plant.

Non-fuel Operating Costs

Solaris and CE estimated non-fuel-operations and maintenance (O&M) unit by unit, relying on industrial experience with similar equipment, and with separate estimates

made for first and N^{th} plant designs (Table 2). Variable O&M costs include water, labor, and make-up chemicals. We use a water cost of 0.1 $/m^3, the average water acquisition cost for manufacturing in Canada. Water costs are highly variable, but as an upper bound, seawater desalination at a cost of 1 $/m^3 would only add roughly 5 $/t$CO_2$ to variable O&M. Fixed O&M is dominated by labor costs, and fixed O&M dominates total O&M so, for simplicity, we report the sum of fixed and variable O&M in Table 2 using a utilization, *U*, of 90%.

Levelized Costs

The levelized costs per ton CO_2 captured from the atmosphere are the sum of levelized capital cost, non-fuel-O&M, and energy costs. The levelized capital cost is $CI \times CRF/U$, where capital intensity (*CI*) is the capital cost per unit capacity, e.g., $/t-$CO_2$-year.

The capital recovery factor (*CRF*) is a levelized annual charge on capital divided by the overnight capital cost. If interest on debt is 5%, for example, and return on equity capital is 12.5% then the weighted average cost of capital is 8% for a project with 60% debt financing, yielding a *CRF* of 9.4% if the project is amortized over 25 years. Actual project finance uses a more complex financial structure and includes taxes, but for a rough engineering-economic estimate we reduce all financial uncertainties to variation in the *CRF*. Table 2 presents results for *CRF*s of 7.5% and 12.5%

The final factor is energy costs. These vary sharply around the world. The results in Table 2 assume a natural gas cost of 3.5 $/GJ and use show results for electricity costs of 30 and 60 $/MWhr.

DISCUSSION

Given the potential importance of estimates of DAC cost to climate policy,[3,12,45] we compare our work with prior estimates, discuss life cycle emission, and speculate about the prospects for reducing costs.

Comparison with Prior Estimates

The most influential prior estimate of DAC costs was provided by a 2011 American Physical Society (APS) study.[4] The study estimated the cost of an aqueous Ca-looping technology like that presented here. The APS "realistic" case had costs of 780 $/t-$CO_2$-avoided and 550 $/t-$CO_2$-captured, where the "avoided" value includes emission from electricity supply outside the plant boundary. Our cost range is 94–232 $/t-$CO_2$ captured, and if we use the financial and gas price assumptions of the APS (*CRF* = 12% and 6 $/GJ), then our costs would be 107–249 $/t-$CO_2$ for the A and B variants in Table 2.

What accounts for this difference?

The cost discrepancy is primarily driven by divergent design choices rather than by differences in methods for estimating performance and cost of a given design. Our own estimates of energy and capital cost for the APS design roughly match the APS values. The most important design choices involved the contactor including (1) use of vertically oriented counterflow packed towers, (2) use of Na^+ rather than K^+ as the cation which reduces mass transfer rates by about one-third,[28,46] and (3) use of steel packings which have larger pressure drop per unit surface area than the packing we chose[28] and which cost 1,700 $/m^3, whereas the PVC tower packings we use cost less than 250 $/m^3.

The APS study and a subsequent paper[14] assumed use of hundreds of vertically oriented counterflow packed towers using a design common to post-combustion CCS. This design requires 190 kWhr/t-CO_2 of energy and has a capital intensity of \$1,304 \$/t-CO_2-year. Our comparable contactor cost is 285 \$/t-CO_2-year computed by multiplying the TDFC value in Table 3 by our average ratio of TPC/TDFL. In rough summary, the APS contactor packed tower design yielded a roughly 4-fold higher capital cost per unit inlet area, and also used packing with 6-fold higher cost, and 2-fold larger pressure drop.

The APS contactor design was motivated by concern about the environmental hazard posed by drift from a contactor using cooling-tower components: "If a caustic solution is used to capture CO_2 and the contactor is unenclosed, then the treated air at a large air capture complex can entrain a mist that releases tonnes of caustic solution per day into the environment… the costs to control these mists may be significant, and in some locations permitting may not even be possible."[14] This assumption appears to be incorrect. The measured drift at the outflow of our contactor is well below indoor air quality limits (see section on the Pilot Contactor). Moreover, it is not clear what an "unenclosed" contactor means, since any DAC contactor must exchange air with the atmosphere. Vertical towers specified by the APS commonly use mist eliminators that operate on the same physical principle with very similar specifications to the mist eliminators used in cooling towers and in our design. But vertical towers—especially an array of hundreds—have much higher capital costs per unit volume enclosed than our design based on large-scale cooling towers.

Another important difference in the calciner thermal energy demand, where APS estimated 8.1 GJ/t-CO_2 processed by the calciner compared with our 5.25 GJ/t-CO_2 estimate. Our lower energy demand arises in part from design choices regarding heat integration along with the use of steam slaking. The APS applied a 75% thermal efficiency to results from prior study,[25] but it is unclear what this efficiency derating means as the direct radiative and conductive heat loss from large calciners vessels is minimal.

Finally, the APS estimates of avoided cost assumed that all electricity is supplied from a grid with an emissions intensity of 610 kg-CO_2/MWhr. We agree with the APS assessment that it would make little sense to build a DAC plant driven by electricity from a high-carbon grid. The primary technology variant analyzed here uses no net grid electricity, but even for a system with electricity inputs, the APS estimate is high. Global average emissions intensity[47] was 520 kg-CO_2/MWhr in 2013 and it has likely declined since then, with current US emission intensity[48] falling to 450 kg-CO_2/MWhr. Global intensities would only be relevant in a world with perfect universal electric transmission. In practice, there are many locations where low-carbon renewables are transmission constrained. These are the locations where DAC with electricity imports makes sense. At a 300 kg-CO_2/MWhr grid intensity and with the 0.366 MWhr/t-CO_2 demand of our "C" variant DAC plant, for example, the grid emissions would be 117 kg-CO_2 per ton captured from the atmosphere. This raises the avoided cost only 13% above the CO_2 captured cost. This is not an unreasonable constraint to siting of DAC plants, given that roughly 20% of world's electricity[47] now has an average intensity below 300 kg-CO_2/MWhr.

Avoided Emissions and Life Cycle Accounting

A full assessment of DAC needs to address emissions on a life cycle basis, accounting for emissions from construction, indirect emissions from production of inputs used during operations, disposal of wastes, fugitive emissions, and decommissioning.

Full life cycle assessment (LCA) is far beyond the scope of this paper, which aims to provide a quantitative process description that may serve as an input to LCA. Here we provide some preliminary observations.

In configurations that use electricity, the grid emission intensity will be a major determinant of LCA emissions. Although, as discussed above, the impact of electricity emission on avoided cost can still be comparatively small.

CE has performed an LCA of CO_2 emissions for a pure sequestration configuration like that in Scenario B. We used the Economic Input Output LCA tool[49] to estimate construction phase emissions given construction cost estimates slightly lower than those in Table 3. We used a natural gas emission factor of 63.8 kg-CO_{2e}/GJ-NG for upstream and direct combustion emissions, which is relatively high, and published emissions factors for make-up chemicals and disposal. Fugitive leakage from the DAC facility was combined with estimates for leakage during transport and injection and geological storage. The net result was that ~0.9 tons of CO_2 were permanently sequestered for each ton captured from air.

The results of this LCA are subject to considerable uncertainty, but they are broadly consistent with LCAs for similar large energy projects, which generally find that use-phase emissions are much larger than emissions from construction and decommissioning.

Prospects for Technology Development and Cost Reduction

It is difficult to estimate the cost of a technology prior to its widespread deployment. CE has spent several tens of millions of dollars developing DAC technology, yet our performance and cost estimates still carry substantial uncertainty. Our process design choices were substantially driven by a goal of reducing development risk and reducing the capital cost of early plants, rather than by minimizing energy use or ultimate levelized cost. CE adopted a conservative approach to cost and performance estimation, driven, in part, by controversy around the feasibility and cost of DAC. The process described here should therefore be seen as a low-risk starting point rather than a fully optimized least-cost design.

Many small process changes will incrementally improve performance relative to the baseline described here. Some improvements will be implemented as "de-bottlenecking" measures on early plants, while others can only be in incorporated in the design of new plants. Beyond minor changes to the process described here, CE is developing alternate DAC processes. One process involves an all-electric variant of the calcium cycle that eliminates natural gas input. Another is an all liquid-phase regeneration system developed from CE's membrane-enhanced thermal swing DAC process.[50] These processes are all built on CE's air contactor as a common platform technology, since the cooling-tower derived aqueous contactor provides a low-risk, low-energy, and low-capital cost front end for DAC.

SUPPLEMENTAL INFORMATION

Supplemental Information includes four figures and can be found with this article online at https://doi.org/10.1016/j.joule.2018.05.006.

ACKNOWLEDGMENTS

The authors acknowledge the input of the entire Carbon Engineering team, particularly Adrian Corless, Dan Kahn, Paul Klavins, Jenny McCahill, Kevin Nold, Jane Ritchie, and Anna Stukas. We also thank Evan Sherwin and two anonymous referees for their care

in reviewing the manuscript. Most of the funding for the work reported here came from funds CE raised from its investors. This research was also supported in part by the British Columbia Innovative Clean Energy Fund, Sustainable Development Technologies Canada (contract number 13A-2368), the Industrial Research Assistantship Program, and the U.S. Department of Energy. This material is based upon work supported by the Department of Energy under Award Number DE-FE0026861. This report was prepared as an account of work sponsored by an agency of the United States Government. Neither the United States Government nor any agency thereof, nor any of their employees, makes any warranty, express or implied, or assumes any legal liability or responsibility for the accuracy, completeness, or usefulness of any information, apparatus, product, or process disclosed, or represents that its use would not infringe privately owned rights. Reference herein to any specific commercial product, process, or service by trade name, trademark, manufacturer, or otherwise does not necessarily constitute or imply its endorsement, recommendation, or favoring by the United States Government or any agency thereof. The views and opinions of authors expressed herein do not necessarily state or reflect those of the United States Government or any agency thereof.

AUTHOR CONTRIBUTIONS

Conceptualization: D.W.K., G.H., D.S.A., and K.H. Methodology: D.W.K., G.H., and K.H. Investigation: D.W.K., G.H., and K.H. Resources: G.H. and K.H. Writing – Original Draft: D.K. and G.H. Visualization: G.H. and K.H. Supervision: D.W.K. and D.S.A. Project Administration: D.S.A. Funding Acquisition: D.W.K., G.H., and K.H.

DECLARATION OF INTERESTS

All authors are employees of Carbon Engineering. All authors have an ownership stake in the form of shares and/or options. David W. Keith is a founder of Carbon Engineering and serves on its Board. The authors are among the inventors of the following US Patents: US9095813B2, US8119091B2, US8871008B2, US8728428B1, and US9637393B2.

Received: March 16, 2018
Revised: May 3, 2018
Accepted: May 16, 2018
Published: June 7, 2018; corrected online: June 11, 2018; corrected online: September 21, 2018

REFERENCES

1. Beller, M., and Steinberg, M. (1965). Liquid-fuel synthesis using nuclear power in a mobile energy depot system. Trans. Am. Nucl. Soc. *8*.

2. Lackner, K.S., Ziock, H.-J., and Grimes, P. (1999). Carbon Dioxide Extraction from Air: Is it an Option? Technical Report LA-UR-99–583 (Los Alamos National Laboratory).

3. Lackner, K.S. (2016). The promise of negative emissions. Science *354*, 714.

4. Socolow, R., Desmond, M., Aines, R., Blackstock, J., Bolland, O., Kaarsberg, T., Lewis, N., Mazzotti, M., Pfeffer, A., Sawyer, K., et al. (2011). Direct Air Capture of CO_2 with Chemicals: A Technology Assessment for the APS Panel on Public Affairs (American Physical Society).

5. House, K.Z., Baclig, A.C., Ranjan, M., van Nierop, E.A., Wilcox, J., and Herzog, H.J. (2011). Economic and energetic analysis of capturing CO_2 from ambient air. Proc. Natl. Acad. Sci. USA *108*, 20428–20433.

6. Lackner, K.S., Brennan, S., Matter, J.M., Park, A.H., Wright, A., and van der Zwaan, B. (2012). The urgency of the development of CO_2 capture from ambient air. Proc. Natl. Acad. Sci. USA *109*, 13156–13162.

7. Martin, D., Johnson, K., Stolberg, A., Zhang, X., and De Young, C. (2018). Carbon Dioxide Removal Options: A Literature Review Identifying Carbon Removal Potentials and Costs (University of Michigan Energy Institute), Available at: http://energy.umich.edu/research/publications/carbon-dioxide-removal-options-literature-review-identifying-carbon-removal.

8. Sanz-Pérez, E.S., Murdock, C.R., Didas, S.A., and Jones, C.W. (2016). Direct capture of CO_2 from ambient air. Chem. Rev. *116*, 11840–11876.

9. Herzog, H. (2003). Assessing the Feasibility of Capturing CO_2 from the Air (Mass. Inst. Technol. Lab. Energy Environ.), Publ. No LFEE 2.

10. Brandani, S. (2012). Carbon dioxide capture from air: a simple analysis. Energy Environ. *23*, 319–328.

11. Wilcox, J., Psarras, P.C., and Liguori, S. (2017). Assessment of reasonable opportunities for direct air capture. Environ. Res. Lett. *12*, 065001.

12. Pielke, R.A. (2009). An idealized assessment of the economics of air capture of carbon dioxide in mitigation policy. Environ. Sci. Policy *12*, 216–225.

13. Ranjan, M. (2010). Feasibility of Air Capture (Massachusetts Institute of Technology).

14. Mazzotti, M., Baciocchi, R., Desmond, M.J., and Socolow, R.H. (2013). Direct air capture of CO_2 with chemicals: optimization of a two-loop hydroxide carbonate system using a

countercurrent air-liquid contactor. Clim. Change *118*, 119–135.

15. Stolaroff, J.K., Keith, D.W., and Lowry, G.V. (2008). Carbon dioxide capture from atmospheric air using sodium hydroxide spray. Environ. Sci. Technol. *42*, 2728–2735.

16. Zeman, F. (2014). Reducing the cost of Ca-based direct air capture of CO_2. Environ. Sci. Technol. *48*, 11730–11735.

17. Mahmoudkhani, M., Heidel, K.R., Ferreira, J.C., Keith, D.W., and Cherry, R.S. (2009). Low energy packed tower and caustic recovery for direct capture of CO_2 from air. Energy Procedia *1*, 1535–1542.

18. Burhenne, L., Giacomin, C., Follett, T., Ritchie, J., McCahill, J.S.J., and Mérida, W. (2017). Characterization of reactive $CaCO_3$ crystallization in a fluidized bed reactor as a central process of direct air capture. J. Environ. Chem. Eng. *5*, 5968–5977.

19. Keith, D., Heidel, K., and Cherry, R. (2010). Capturing CO_2 from the atmosphere: rationale and process design considerations. In Geo-Engineering Climate Change: Environmental Necessity or Pandora's Box?, B. Launder and J.M.T. Thompson, eds. (Cambridge University Press), pp. 107–126.

20. Wang, T., Lackner, K.S., and Wright, A. (2011). Moisture swing sorbent for carbon dioxide capture from ambient air. Environ. Sci. Technol. *45*, 6670–6675.

21. Lackner, K.S. (2009). Capture of carbon dioxide from ambient air. Eur. Phys. J. Spec. Top. *176*, 93–106.

22. Zeman, F.S., and Lackner, K.S. (2004). Capturing carbon dioxide directly from the atmosphere. World Resour. Rev. *16*, 157–172.

23. Holmes, G., and Keith, D. (2012). An air-liquid contactor for large-scale capture of CO_2 from air. Philos. Trans. A Math. Phys. Eng. Sci. *370*, 4380–4403.

24. Rickover, H. (1953). Letter. Available at: http://ecolo.org/documents/documents_in_english/Rickover.pdf. Accessed 10 January, 2018.

25. Baciocchi, R., Storti, G., and Mazzotti, M. (2006). Process design and energy requirements for the capture of carbon dioxide from air. Chem. Eng. Process. Process Intensif. *45*, 1047–1058.

26. Heidel, K.R., Ritchie, J.A., Kainth, A.P.S., and Keith, D.W. (2014). United States Patent: 8728428-Recovering a caustic solution via calcium carbonate crystal aggregates. Filed March 13, 2013, and issued May 20, 2014.

27. Heidel, K.R., Keith, D.W., Ritchie, J.A., Vollendorf, N., and Fessler, E. (2017). United States Patent: 9637393-Recovering a caustic solution via calcium carbonate crystal aggregates. Filed May 19, 2014, and issued May 2, 2017.

28. Holmes, G. (2010). A Carbon Dioxide Absorption Performance Evaluation for Capture from Ambient Air (University of Calgary).

29. Tepe, J.B., and Dodge, B.F. (1943). Absorption of carbon dioxide by sodium hydroxide solutions in a packed column. Trans. Am. Inst. Chem. Eng. *39*, 255–276.

30. Spector, N.A., and Dodge, B.F. (1946). Removal of carbon dioxide from atmospheric air. Trans. Am. Inst. Chem. Eng. *42*, 827–848.

31. Danckwerts, P.V., Kennedy, A.M., and Roberts, D. (1963). Kinetics of CO_2 absorption in alkaline solutions—II: absorption in a packed column and tests of surface-renewal models. Chem. Eng. Sci. *18*, 63–72.

32. Astarita, G. (1966). Regimes of mass transfer with chemical reaction. Ind. Eng. Chem. *58*, 18–26.

33. Zeman, F. (2007). Energy and material balance of CO_2 capture from ambient air. Environ. Sci. Technol. *41*, 7558–7563.

34. Keith, D., Mahmoudkhani, M., Biglioli, A., Hart, B., Heidel, K., and Foniok, M. (2015). United States Patent: 9095813. Carbon dioxide capture method and facility. Filed August 21, 2009, and issued August 4, 2015.

35. Faust, S.D., and Aly, O.M. (1998). Chemistry of Water Treatment, Second Edition (CRC Press).

36. Lassiter, J., and Misra, S. (2013). Carbon Engineering (Harvard Business School).

37. Pröll, T., Rupanovits, K., Kolbitsch, P., Bolhàr-Nordenkampf, J., and Hofbauer, H. (2009). Cold flow model study on a dual circulating fluidized bed (DCFB) system for chemical looping processes. Chem. Eng. Technol. *32*, 418–424.

38. Heidel, K.R. and Rossi, R.A.. United States Patent application: 0170327421. High Temperature Hydrator (A1). Filed May 10, 2017, and issued A1.

39. Zeman, F.S., and Keith, D.W. (2008). Carbon neutral hydrocarbons. Philos. Trans. A Math. Phys. Eng. Sci. *366*, 3901–3918.

40. Holmes, G., Nold, K., Walsh, T., Heidel, K., Henderson, M.A., Ritchie, J., Klavins, P., Singh, A., and Keith, D.W. (2013). Outdoor prototype results for direct atmospheric capture of carbon dioxide. Energy Procedia, 6079–6095, https://doi.org/10.1016/j.egypro.2013.06.537.

41. CDC - NIOSH pocket guide to chemical hazards—potassium hydroxide. Available at: https://www.cdc.gov/niosh/npg/npgd0523.html.

42. Gebald, C., Wurzbacher, J.A., Tingaut, P., and Steinfeld, A. (2013). Stability of amine-functionalized cellulose during temperature-vacuum-swing cycling for CO_2 capture from air. Environ. Sci. Technol. *47*, 10063–10070.

43. KBR. Front end loading process. Available at: https://www.kbr.com/Documents/Onshore%20Refining%20Handouts/FrontEndLoadingProcessAndDeliverables_final.pdf.

44. Rubin, E.S., Short, C., Booras, G., Davison, J., Ekstrom, C., Matuszewski, M., and McCoy, S. (2013). A proposed methodology for CO_2 capture and storage cost estimates. Int. J. Greenh. Gas Control *17*, 488–503.

45. Smith, P., Davis, S.J., Creutzig, F., Fuss, S., Minx, J., Gabrielle, B., Kato, E., Jackson, R.B., Cowie, A., Kriegler, E., et al. (2016). Biophysical and economic limits to negative CO_2 emissions. Nat. Clim. Change *6*, 42–50.

46. Pohorecki, R., and Moniuk, W. (1988). Kinetics of reaction between carbon dioxide and hydroxyl ions in aqueous electrolyte solutions. Chem. Eng. Sci. *43*, 1677–1684.

47. Ang, B.W., and Su, B. (2016). Carbon emission intensity in electricity production: a global analysis. Energy Policy *94*, 56–63.

48. CMU. US Power Sector Emissions. CMU Power Sector Carbon Index (2018). Available at: https://emissionsindex.org/.

49. Carnegie Mellon University Green Design Institute. Economic Input-Output Life Cycle Assessment (EIO-LCA), US 1997 Industry Benchmark model. (2008). Available at: http://www.eiolca.net/.

50. Henderson, M.A., Keith, D.W., Kainth, A.P.S., Heidel,K.R., and Ritchie, J.A. (2014). United States Patent: 8871008. Target gas capture. Filed September 7, 2012, and issued October 28,2014.